

Chemistry–A European Journal

Supporting Information

Study of the Lithium Storage Mechanism of N-Doped Carbon-Modified Cu₂S Electrodes for Lithium-Ion Batteries

Guiying Tian, Chuanfeng Huang, Xianlin Luo, Zijian Zhao,* Yong Peng, Yuqin Gao, Na Tang, and Sonia Dsoke*

Supporting Information

Experimental Section

Synthesis of CuS/C via co-precipitation

CuS nanoparticles were synthesized via a co-precipitation method. $\text{Cu}(\text{NO}_3)_2 \cdot 3\text{H}_2\text{O}$ ($\geq 98.0\%$, Sigma-Aldrich) and thioacetimidic acid ($\text{C}_2\text{H}_5\text{NS}$, $\geq 99.0\%$, Sigma-Aldrich) were used in Cu:S molar ratio of 1.0:1.1. $\text{Cu}(\text{NO}_3)_2$ was firstly dissolved in deionized water. Afterwards, 10 wt.% thioacetimidic acid aqueous solution was dropwise added into the boiling 0.5M $\text{Cu}(\text{NO}_3)_2$ solution with vigorous stirring. The sediment, formed via an electrostatic assembly, was washed and centrifuged several times with deionized water and ethanol. After drying at 80 °C for 12 h, a black CuS precursor was obtained. A part of CuS precursor was calcinated at 500 °C for 3 h under argon flow, denoted as CuS. The rest of the CuS precursor was modified via the carbon loading method (see next session 2.2).

Synthesis of $\text{Cu}_2\text{S/C}$ via thermal reduction

Based on the previous report,^[1] 0.50 g CuS precursor was dispersed in 100 mL deionized water to form a homogeneous suspension. Then, 1.25 g poly(diallyldimethylammonium chloride) (PDDA, 20 wt.%, $M_w < 500000$ Da, Aldrich) and 0.84 g poly(sodium-4-styrenesulfonate) (PSS, 30 wt.%, $M_w < 70000$ Da, Aldrich) were respectively dispersed in the suspension under vigorous stirring. The obtained sediment was washed and carbonized at 500 °C for 3 h under argon flow, denoted as $\text{Cu}_2\text{S/C}$.

General materials characterization

Raman test was performed by a Raman spectrometer (LabRam Evolution HR, HORIBA Jobin Yvon) using 633 nm laser. XRD test was employed using an STOE STADI P X-ray powder diffractometer equipped with a Mythen1K detector and a Mo $\text{K}_{\alpha 1}$ radiation ($\lambda = 0.70932$ Å) in a 2θ range of $10^\circ \sim 50^\circ$ in Debye–Scherrer geometry. Rietveld refinement was performed to analyze the diffraction data using FullProf software^[2]. A field-emission scanning electron microscope (SEM, Merlin Carl Zeiss) was used to characterize the sample morphology. Energy-dispersive X-ray spectroscopy (EDX, Bruker, Quantax 400 SDD) was used to determine the elemental composition. X-ray photoelectron spectroscopy (XPS) was performed on a K-Alpha XPS instrument (Thermo-Fisher Scientific, East Grinstead). The K-Alpha charge compensation system was used to prevent any local charge buildup. All samples were analyzed using a monochromated Al K_{α} X-ray source (400 μm spot size). The spectra are referenced in binding energy to the C 1s peak (C–C, C–H) at 285 eV binding energy.

Operando test using synchrotron radiation diffraction

To monitor the phase evolution of the $\text{Cu}_2\text{S/C}$ precursor during the thermal reduction process, *operando* high-temperature synchrotron radiation powder diffraction (HT-SRD) was employed at P02.1, DESY PETRA-III, Germany, using monochromatic synchrotron diffraction ($\lambda = 0.20737(4)$ Å). Here, NaCl and LaB_6 were used as standard samples for the calibration of temperature and wavelength. The $\text{Cu}_2\text{S/C}$ precursor was sealed in a quartz capillary under argon atmosphere and heated with a heating rate of 20 °C min^{-1} up to 800 °C. The as-obtained 2D image data were transformed to intensity- 2θ data using Fit2D software.^[2] Also, *in situ* X-ray absorption spectroscopy (XAS) spectra were collected in transmission geometry with the step-scan mode at the Cu K-edge (8979 eV). The Si(111) double-crystal monochromator equipped with a ionization chamber was optimized for the Cu edge absorption. Here, coin cells with glass windows ($\text{Li}||\text{LP30}||\text{Cu}_2\text{S/C}$) were assembled. The working electrodes were prepared by mixing $\text{Cu}_2\text{S/C}$ (70 wt.%), carbon black (20 wt.%, Super P Li, Timcal Ltd.) and polytetrafluoroethylene (10 wt.%, PTFE beads, Aldrich), and then loaded on the steel mesh disk (ϕ 12 mm) as current collector. The cell was discharged at a current density of 100 mA g^{-1} in a potential range of 0.01–3.0 V vs. Li/Li^+ .

To understand the mechanism of lithium storage in the $\text{Cu}_2\text{S/C}$, *operando* SRD data were collected at the MSPD beamline, ALBA, Spain using synchrotron radiation ($\lambda = 0.41311(2)$ Å). LaB_6 was used as a standard sample for wavelength calibration. Coin cells with glass windows ($\text{Li}||\text{LP30}||\text{Cu}_2\text{S/C}$) were assembled. The working electrodes were prepared by mixing 70 wt.% $\text{Cu}_2\text{S/C}$. The mixture (~3.5 mg) was pressed on a copper mesh disk (ϕ 12 mm). During the *operando* SRD test, the cell was cycled at 60 mA g^{-1} in a potential range of 0.01–3.0 V vs. Li/Li^+ at room temperature.

Electrochemical characterization

The working electrodes were made of $\text{Cu}_2\text{S/C}$ (70 wt.%), carbon black (20 wt.%) and PVDF binder (10 wt.%, R6020/1001, Solvay). The as-prepared homogeneous slurry was coated on a copper foil. The coated foils were dried in a fume hood for 2 h and then dried at 80 °C for 12 h to completely remove N-methyl pyrrolidone solvent. Afterward, the coated foils were punched into circular electrodes (ϕ 12 mm) with mass loading of 1.5–1.8 mg cm^{-2} $\text{Cu}_2\text{S/C}$ and a drying thickness of ~12.2 μm . The assembled LIB coin cell (CR2032 type) consists of a working electrode, a Whatman® glass-fiber separator (ϕ 17 mm), a lithium foil (ϕ 15 mm, Alfa Aesar) and 180 μL of LP30 electrolyte (1 M LiPF_6 in ethylene carbonate/dimethyl carbonate = 1:1

by mass ratio, BASF). All cells were assembled in an argon-filled glovebox (MB200, MBraun GmbH). During the electrochemical tests, the cells were kept in a climate chamber (Binder GmbH) at 25 °C. Galvanostatic charge/discharge (GCD) and cyclic voltammetry (CV) were employed using a Bio-Logic VMP3 potentiostat in a potential range of 3.0 to 0.01 V vs. Li/Li⁺.

Discussion Section

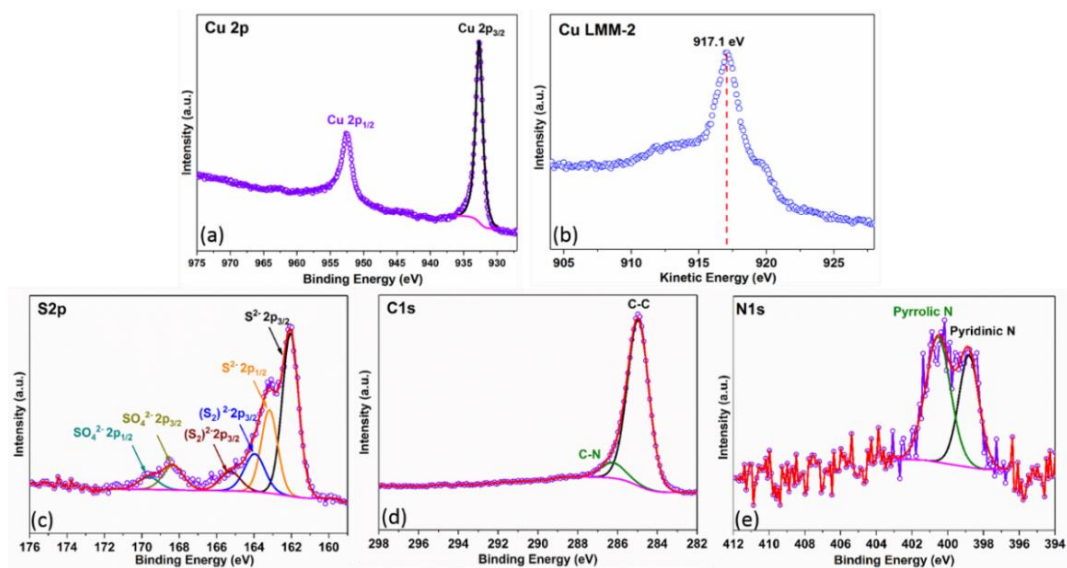


Figure S1. XPS spectra of pristine $\text{Cu}_2\text{S}/\text{C}$: Cu 2p (a), Cu LMM-2 (b), S 2p (c), C 1s (d), and N 1s (e).

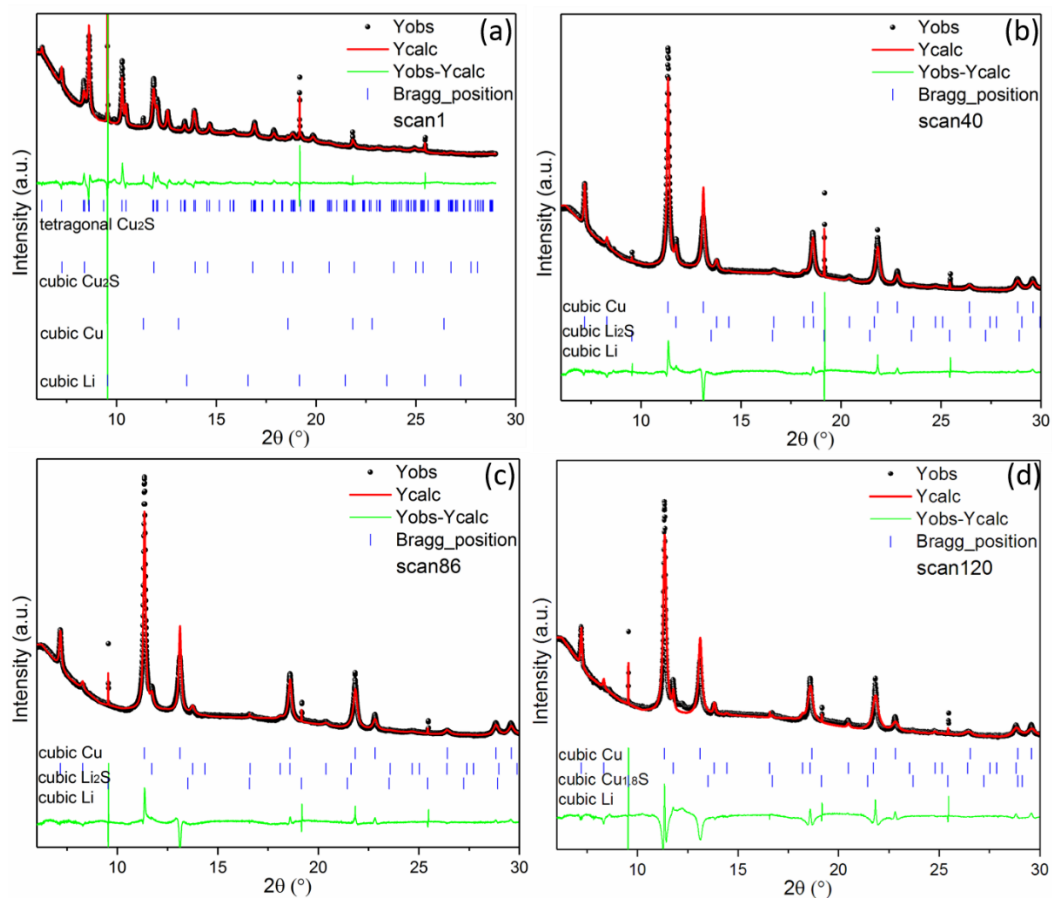


Figure S2. Analysis of typical phase change of the $\text{Cu}_2\text{S}/\text{C}$ electrode in LIBs based on Rietveld refinement: (a) step A–scan1, (b) step B–scan40, (c) step C–scan86, and (d) step D–scan120.

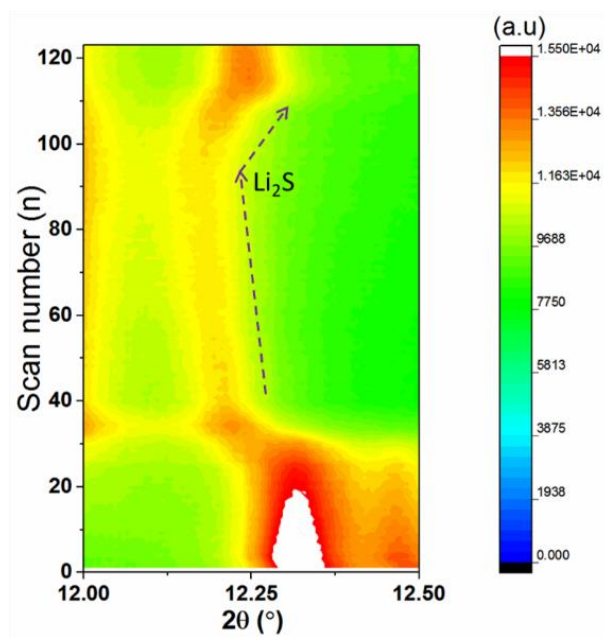


Figure S3. *Operando* SRD analysis of the Li₂S reflection in Cu₂S/C electrode.

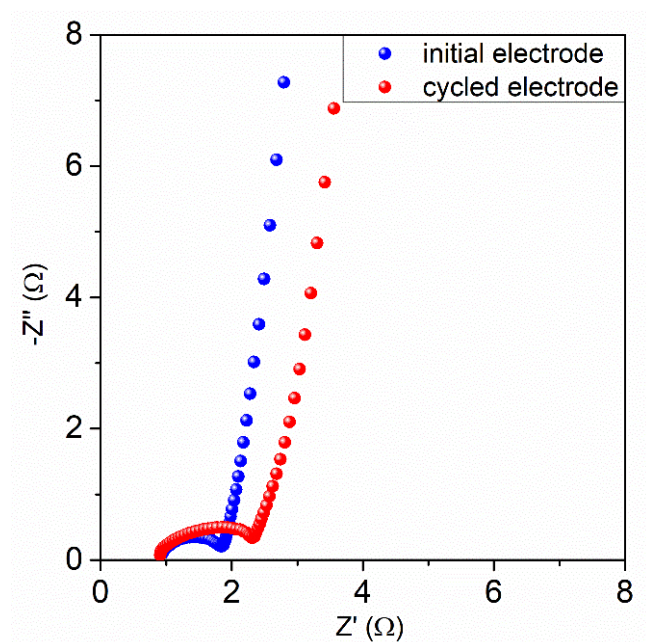


Figure S4. Nyquist plots obtained from the EIS test of the $\text{Cu}_2\text{S}/\text{C}$ composite electrode before and after the first cycle at 60 mA g^{-1} in a potential range of $0.01\sim 3.0 \text{ V}$ vs. Li/Li^+ at room temperature.

Table S1. A review of preparation methods of Cu₂S and Cu₂S/carbon composite, and corresponding electrochemical performance for LIBs.

sample	Cu ₂ S preparation	Cu ₂ S morphology	compositing method	specific capacity	initial coulombic efficiency	year
Cu ₂ S ^[3]	hydrothermal approach	particles (~500 nm)	–	0.27 mAh cm ⁻² at 100 cycles at 0.1 mA cm ⁻²	99.4%	2012
Cu ₂ S ^[4]	hydrothermal method	particle cluster	–	~25 mAh g ⁻¹ at 0.1 A g ⁻¹ after 100 cycles	83%	2015
Cu ₂ S ^[5]	precipitation	spherical particles (~0.4 μm)	–	~220 mAhg ⁻¹ at 1C over 100 cycles	~100%	2016
Cu ₂ S ^[6]	hydrothermal approach	nanorods	–	164.8 mAh g ⁻¹ after 150 cycles at 0.2A g ⁻¹	53.7%	2018
Cu ₂ S ^[7]	hydrothermal method	flower–likes	–	~300 mAh g ⁻¹ at 0.1 A g ⁻¹ after 200 cycles	~62%	2020
Cu ₂ S/CuS ^[8]	commercially available	rods (~3 mm in diameter and 6 mm in length)	mechanical stirring	~200 mAh g ⁻¹ at 1C for over 150 cycles	>98.4%	2014
Cu ₂ S/tubular mesoporous carbon ^[9]	in situ electrochemical corrosion	Cu ₂ S/tubular mesoporous carbon composite	direct growth of Cu ₂ S nanowire on a Cu film	270 mA h g ⁻¹ at 0.2C after 300 cycles	92 %	2014
Cu ₂ S/carbon composites ^[4]	hydrothermal method	particle cluster	calcination with glucose	300 mAh g ⁻¹ after 100 cycles at 0.1A g ⁻¹	72%	2015
Cu ₂ S@ N, S-doped carbon ^[6]	hydrothermal approach	nanorods	in-situ polymerization and carbonization with pyrrole	560 mAh g ⁻¹ at 1A g ⁻¹ after 550 cycles	62.4 %	2018
Cu ₂ S@rGO ^[7]	hydrothermal method	flower–likes (thickness ~20nm)	freeze–drying process	600 mAhg ⁻¹ after 200 cycles at	98%	2020

0.1 Ag ⁻¹						
Cu ₂ S/C ^[10]	spray-dried	~10 nm particles	co-calcination with glucose	250 mAh g ⁻¹ at 0.2 A g ⁻¹ after 100 cycles	> 98%	2020
Cu ₂ S/N-doped carbon ^{this work}	precipitation	~90 nm particles	co-calcination with polyelectrolytes	523 mAh g ⁻¹ at 0.1 A g ⁻¹ at the 200th cycle	57.9%	2021

References

- [1] G. Tian, F. Scheiba, L. Pfaffmann, A. Fiedler, V. S. K. Chakravadhanula, G. Balachandran, Z. Zhao, H. Ehrenberg, *Electrochim. Acta* **2018**, 283, 1375–1383.
- [2] J. Rodríguez-Carvajal, *Phys. B Condens. Matter* **1993**, 192, 55–69.
- [3] S. Ni, T. Li, X. Yang, *Thin Solid Films* **2012**, 520, 6705–6708.
- [4] Y. Liu, B. Jin, Y. F. Zhu, X. Z. Ma, X. Y. Lang, *Int. J. Hydrogen Energy* **2015**, 40, 670–674.
- [5] G. Kalimuldina, I. Taniguchi, *J. Power Sources* **2016**, 331, 258–266.
- [6] Q. Chen, M. Ren, H. Xu, W. Liu, J. Hei, L. Su, L. Wang, *ChemElectroChem* **2018**, 5, 2135–2141.
- [7] X. Zhang, L. Duan, X. Zhang, X. Li, W. Lü, *J. Alloys Compd.* **2020**, 816, 152539.
- [8] B. Jache, B. Mogwitz, F. Klein, P. Adelhelm, *J. Power Sources* **2014**, 247, 703–711.
- [9] F. Han, W. C. Li, D. Li, A. H. Lu, *ChemElectroChem* **2014**, 1, 733–740.
- [10] Y. Wang, X. Feng, Y. Xiong, S. Stoupin, R. Huang, M. Zhao, M. Xu, P. Zhang, J. Zhao, H. D. Abruña, *ACS Appl. Mater. Interfaces* **2020**, 12, 17396–17405.